Design of an ECG front-end considering ST segment distortion

Béatrice Guénégo, Caroline Lelandais-Perrault, Emilie Avignon-Meseldzija, Gérard Sou, Philippe Benabes

Design of an ECG front-end considering ST segment distortion

Béatrice Guénégo*, Caroline Lelandais-Perrault*, Émilie Avignon-Meseldzija*, Gérard Sou†, Philippe Bénabès*
*Université Paris-Saclay, CentraleSupélec, CNRS, Laboratoire de Génie Électrique et Électronique de Paris
91192 Gif-sur-Yvette, France
†Sorbonne Université, CNRS, Laboratoire de Génie Électrique et Électronique de Paris, 75252, Paris, France
Email: {beatrice.guenego, caroline.lelandais-perrault, emilie.avignon, philippe.benabes}@geeps.centralesupelec.fr
gerard.sou@sorbonne-universite.fr

***Abstract*—ECG ST segment should be monitored for myocardial ischemia diagnosis. But this information needs a very accurate ECG acquisition. This paper presents the design of a chopper amplifier filtering the baseline wander and minimizing the added electronic noise with an acceptable ST segment distortion. A method is proposed to estimate the ST segment distortion and compare it to the International Electrotechnical Commission (IEC) standards. The design is achieved using XFAB 180nm technology and validated at transistor-level simulation for typical and worst cases.**

***Keywords*—Electrocardiogram (ECG), Chopper Amplifier, Myocardial Ischemia, Signal Distortion, ST segment, Embedded baseline wander elimination**

I. Introduction

According to the World Health Organization, ischemic heart diseases are the leading death cause worldwide [1]. Myocardial ischemia is due to a reduced and insufficient blood supply to the heart, altering its functioning and eventually leading to myocardial infarction. Diagnosis is generally realized with an electrocardiogram (ECG) measured on the patient torso, which gives an image of the heart's electric activity. ECGs are usually measured at the hospital, at the cardiologist's, or by emergency services, but they can also be recorded at home for several days before being presented to the practitioner.

However, there is a need for continuous monitoring systems, which could be worn all day and would raise warnings in case of ischemic events. These systems would include embedded processing and classification between healthy and pathologic events. They should extract meaningful features for the diagnosis from the ECG. For example, arrhythmias (heart rhythm-related pathologies) require peak detection and time interval measurements. On the other hand, ischemia diagnosis requires a more precise morphology analysis, including measures of the level difference between two segments of the ECG beat.

Embedded ECG processing and feature extraction raise many challenges. ECGs are subject to noises related to regular human activity (breathing, movements, etc.). It makes signal acquisition and denoising critical steps to ensure a reliable diagnosis with on-chip measurements. These two steps should be realized without ECG distortions that can put the reliability of the diagnosis into question even if the digital processing is flawless. The International Electrotechnical Commission (IEC) has issued standards to guide ECG measurement systems design [2].

Embedded systems for measuring and processing ECG presented in recent papers focus on cardiac arrhythmias. Therefore, the vast majority ignore the issue of ECG morphology distortion and do not fulfill standards requirements. References [3], [4] propose ECG chips that detect peaks or slope thresholds. They focus on classifying healthy or arrhythmic beats and use aggressive analog filtering to emphasize peaks. Reference [5] detects arrhythmias using digital neural networks. Some others present ECG analog front-ends (AFE) without assessing distortion [6], [7]. References [8]–[10] address ECG distortion. However, the first one focuses on the distortion linked to electrodes. The others focus on digital noise processing but do not deal with the analog part. Therefore, a proper estimation of distortion introduced by analog ECG processing is needed to validate that systems are adapted to ischemia [11].

This paper seeks to prove the feasibility of an AFE dedicated to ST segment analysis and baseline removal by sizing a circuit that does not compromise ECG medical information. For this purpose, a distortion quantification method and a circuit minimizing the flicker noise have been designed to ensure the introduced distortion is lower than the standard's maxima. The design has been achieved using XFAB 180nm technology. Simulation results show distortion below the standard recommendations even in worst-case simulations.

Sec. II focuses on the ECG and standards used as references. Sec. III presents the distortion estimation method. Sec. IV describes the architecture and the transistors sizing. The simulation results are presented in Sec. V.

II. ECG and Distortions Standards

A. ECG and Ischemia Features

The electrocardiogram (ECG) is a heart electrical activity measurement. This activity is linked to its contraction. The ECG is measured with electrodes placed on the limbs and the torso. The viewpoint on the heart depends on the set of positions chosen, named lead. Even if an ischemia diagnosis requires several leads, this article uses only lead II-like ECGs since the encountered difficulties are the same for one or many leads. Moreover it is the one used by the norm described hereafter. The morphology is illustrated in Fig. 1.

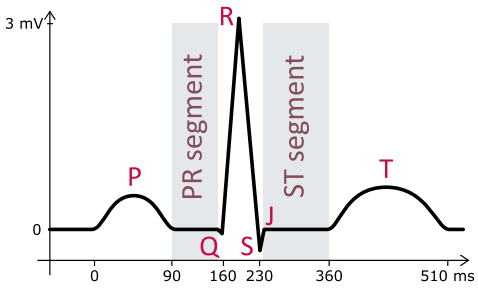

Fig. 1. Electrocardiogram, lead II, with typical amplitude and time values

The physiological rhythm shows three significant events: the P wave, the QRS complex, and the T wave. They are linked to, respectively, atrial contraction, ventricular contraction, and ventricular relaxation. The distance between successive R-peaks is used to compute the cardiac rhythm, which is between 60 and 100 beats per minute (bpm). The PR and ST segments are defined in between those waves. If the beat is physiological, the ST segment should be isoelectric, which means it should be on the same level as the PR segment. The main features to consider for ischemia diagnosis are the deviation of the ST segment from the isoelectric line and the shape of the T wave [12]. Deviations of more than 50μV may raise warnings, especially when they last for some minutes [10].

B. Noises and ECG Distortion Standards

Usually, an ECG is measured at rest and by trained practitioners. It limits noises due to the patient's movements and allows the use of large computers with high computational power and precisely placed and adapted electrodes. When it comes to embedded and daily-life measurement, noise processing becomes challenging because of size and power budget constraints. Indeed the ECG is noisier than at rest, and the computing power is limited.

Electronic noises are a first constraint. The AFE design must minimize those so medical information is not lost. A second constraint is the Baseline Wandering (BW). It is a high amplitude low-frequency noise (from DC offset up to a few Hertz) linked, for example, to breathing or moving cables and electrodes [9]. It should be filtered to minimize analog-to-digital converter (ADC) constraints. Otherwise, the ADC would require many bits to cover the whole voltage range of signal and noise with the target precision for the ECG. Since lower ECG frequencies are around the heart rhythm, a high pass cut-off frequency lower than 0.5Hz is supposed to remove most of the BW. However, filtering easily distorts the ST segment resulting in a trade-off between BW elimination and distortion introduced.

The International Electrotechnical Commission (IEC) has issued recommendations about this matter [2]. It defines maximum distortion levels. The system should not introduce a slope of more than 0.05mV/s in the ST segment and an amplitude difference of more than 25μV for given calibration signals. Those signals have to be used to test the adequation of the design to this standard. Only one of them is shown here to preserve figure readability.

III. Distortion Estimation Method

The distortion introduced by analog processing should be measured for an ischemia embedded monitoring system to be trusted. Fig. 2 illustrates the proposed method to estimate the distortion on the ST segment. The measurement block is adapted to the chosen metric: ST level or ST slope. IEC standard gives reference signals. CAL20100 was chosen. The sampling frequency of calibration signals is 20kHz. *Ref*, the reference signal, and *In*, the same signal processed by the system, are processed in parallel by a MATLAB script. It resynchronizes *Ref* and *In* using R-peaks by adding a delay on *Ref*. Then, it normalizes *In* to the amplitude of *Ref*. Both signals can be compared beat per beat at the end of the normalization stage. Time intervals between segments' bounds and R peaks are fixed variables of the script. The baseline is interpolated from the PR segment. The ST segment is approximated by a linear interpolation, such as the one used for the PR segment, to make the slope estimation more resilient to noise. Then the ST segment level and slope are compared to this baseline. Finally, the error is computed by differentiating both channels' outputs. Fig. 3 illustrates the methodology with a C-R high-pass filtered ECG. The digital processing part would realize the baseline interpolation and ST segment measurements in a complete ischemia embedded monitoring system instead of the script. The linear interpolation from the PR segment is a simple method for baseline estimation. It has been chosen because it assumes simple digital processing that could be implemented on any embedded circuit without requiring complex algorithms or significant computing power.

IV. Proposed Analog Front End Architecture

Several AFE architectures have been proposed in the literature to address biomedical signals and, more specifically, ECG measurement [3], [4], [6], [7], [13]. In the case of ischemia monitoring, the architecture should not distort the ST segment because of the baseline filtering. It should also not introduce electronic noise (thermal or flicker) preventing the digital processing from retrieving the ST segment level and slope.

Preliminary simulations have concluded that 0.03Hz is a sufficiently low enough high-pass cut-off frequency. A higher one would distort the ST segment more than the IEC standard allows. A chopper architecture was chosen to mitigate the flicker noise (1/f noise) because ECG information is concentrated in low frequencies.

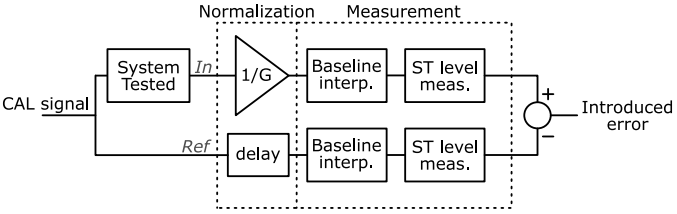

Fig. 2. Distortion estimation flow

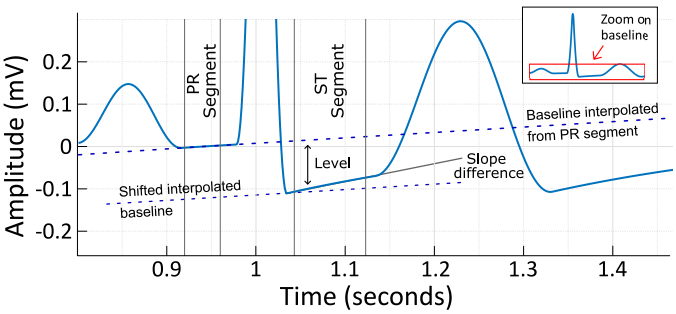

Fig. 3. ST segment distortion measurements on a C-R high-pass filtered ECG beat with $f_{hp} = 0.5$Hz

A. Chopper Instrumentation Amplifier

A Chopper amplifier transposes the signal to the chopping frequency, where the flicker noise is reduced, before amplification. The architecture, shown in Fig. 4, is inspired by [13]. The gain is fixed by the capacitance ratio C_i/C_{hp} as long as the open loop gain is greater than 100dB. The architecture of the two operational transconductance amplifiers (OTA) and the Operational Amplifier (OpAmp) are shown in Fig. 5. The common mode feedback circuits (CMFB) are dual differential pairs as proposed in [14]. C_m and R_m are Miller capacitor and resistor added to ensure a phase margin greater than 60 degrees. A DC servo loop (DSL) suppresses the baseline. It uses an integrator that sets the circuit's high-pass frequency f_{hp} (1). To reach a low high-pass cut-off frequency, R_{int} and C_{int} will be large. In this paper, they are considered as off-chip components.

$$f_{hp} = \frac{1}{2\pi R_{int} C_{int}} \cdot \frac{C_{hp}}{C_{fb}} \tag{1}$$

B. Transistor Level Design

The XFAB 180nm (xh018) technology was chosen. The chopping frequency is 10kHz The closed-loop gain is fixed to 100 with $C_i = 12$pF and $C_{fb} = 120$fF. With C_{hp} equal to C_{fb}, f_{hp} is fixed to 0.03Hz with $R_{int} = 500G\Omega$ and $C_{int} = 10.6$pF. Components C_i, C_{hp}, C_{fb}, and C_m are double metal-metal capacitors, while R_m is a poly resistor. The input

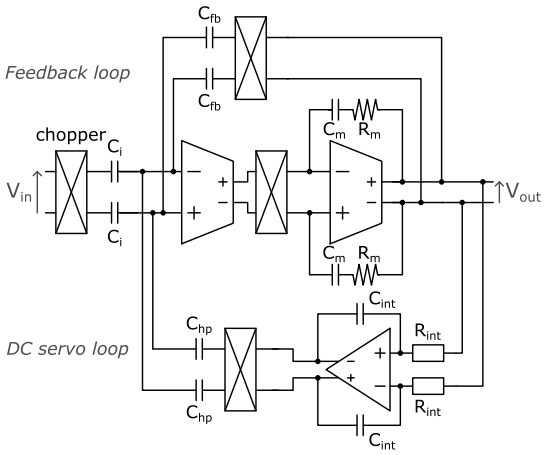

Fig. 4. Chopper-based instrumentation amplifier schematic

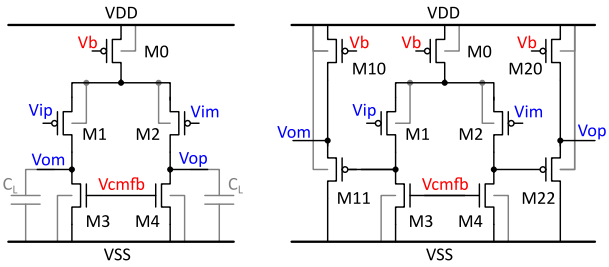

Fig. 5. Schematics of the OTA (left) and the OpAmp (right)

referred flicker noise in an OTA is given by (2), K being the flicker noise constant of the transistor. The thermal noise is given by (3) [14].

$$v^2_{flick}(f) = \frac{2}{C_{ox} \cdot f}\left(\frac{K_{1,2}}{W_{1,2}L_{1,2}} + \frac{\mu_n}{\mu_p} \cdot \frac{K_{3,4}L_{1,2}}{W_{1,2}L^2_{3,4}}\right) \tag{2}$$

$$v^2_{therm}(f) = 2kT\gamma\left(\frac{1}{g_{m1,2}} + \left(\frac{g_{m3,4}}{g_{m1,2}}\right)^2 \cdot \frac{1}{g_{m3,4}}\right) \tag{3}$$

The sizes of transistors $M_{1,2}$ of the OTAs are 200μm/15μm, and the transistors $M_{3,4}$ are 6μm/10μm. Those sizes are large to minimize flicker noise according to (2). The transconductance g_{m1} of the differential pair is high to provide a large gain, which also reduces thermal noise when combined with a small $g_{m3,4}$ according to (3). The sizing of the OpAmp has been done the same way. All sizes are given in Table I. One chopper is made from four transmission gates with minimal-size transistors.

Power consumption is a major concern in embedded circuits but was not prioritized before the distortion issue here. It was minimized until noise prevented correct ST segment information recovery. The supply voltage is 1.8V, and total power consumption is about 29μW.

V. Simulation Results

This circuit has been simulated, with Cadence Virtuoso, in transient with and without noise to assess the distortion introduced by the circuit's transfer function and electronic noises. Twenty heartbeats are simulated. The first ten of them are discarded to eliminate the transient behavior of the high-pass filter. Since the ECG information lies below 200Hz, the transient output signal is low-pass filtered at 250Hz. It

TABLE I
Components Sizing

Component	Size	OpAmp	
C_i	12pF	$M_{1,2}$	120μm/8μm
C_{fb}	120fF	$M_{3,4}$	1μm/6μm
C_{hp}	120fF	$M_{11,22}$	3μm/1μm
C_{int}	10.6pF	M_0	2μm/1μm
R_{int}	500GΩ	$M_{10,20}$	2μm/1μm
C_m	10pF	**OTA**	
R_m	70kΩ	$M_{1,2}$	200μm/15μm
		$M_{3,4}$	6μm/10μm
		M_0	2μm/1μm

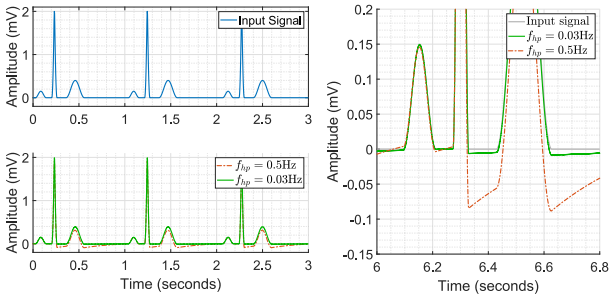

Fig. 6. Noiseless outputs for $f_{hp} = 0.03$ and 0.5Hz

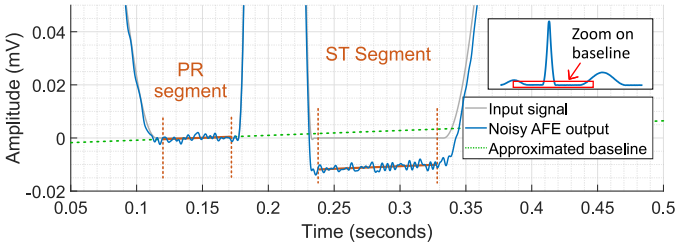

Fig. 7. Effects of noise on the baseline interpolation from PR segment

also removes chopping artifacts. As explained in Sec. III, the baseline is interpolated from the PR segment.

Noiseless simulations demonstrate f_{hp} choice's importance for ST segment measurements (Fig. 6). A 0.5Hz f_{hp}, as in [13], introduces a mean ST level deviation of 83μV and a mean ST slope of 0.17mV/s, which are above the standard requirements. In contrast, a 0.03Hz f_{hp} introduces level and slope distortions below 7.3μV and 0.001mV/s, respectively, which are convenient with IEC standards.

Noise simulations have been realised to assess the introduced distortion and in design worst cases. Fig. 7 highlights the baseline estimation degradation introduced by the noise. The resulting distortion performances are evaluated with corners simulations with noise. Results are summarized in Table II. The worst case is obtained for slow and the best for fast PMOS transistors. Maxima are consistently below the IEC standard requirements for the mean and the maximum deviation values over ten beats.

VI. Conclusion

This work presents a chopper amplifier design dedicated to embedded continuous ischemia monitoring systems based on the ST segment. A distortion estimation method has also been proposed to assess the system's adequacy with IEC standards. The chopper amplifier architecture has been chosen to reduce the impact of flicker noise. The high-pass cut-off frequency used to eliminate baseline wander noise of the ECG is fixed at 0.03Hz. This value is low enough to ensure the circuit's transfer function does not introduce prohibitive ST segment distortion. Then the transistor sizing was realized to ensure that introduced electronic noises do not create false positives or negatives by skewing the baseline approximation. The design achieves ST segment level and slope deviations lower than

TABLE II
Distortion introduced on the ST segment by the design for worst cases and noise

Mean over 10 beats	**Min.**	**Typ.**	**Max.**	**IEC standard**
Level deviation (μV)	6.54	7.24	7.69	$<25\mu$V
Slope deviation (mV/s)	0.011	0.012	0.013	<0.05mV/s
Max. over 10 beats				
Level deviation (μV)	9.08	10.23	11.25	$<25\mu$V
Slope deviation (mV/s)	0.027	0.032	0.039	<0.05mV/s

8μV and 0.04mV/s in typical and worst cases simulations. Therefore, it respects the 25μV and 0.05mV/s maxima given by the IEC standards. Further work includes an ADC and voltage buffer design and a digital detection of ischemia from the ST segment deviations.

References

[1] W. H. Organization, "The top 10 causes of death," 2020. Accessed: 2022-06-07.

[2] "IEC 60601-2-25 Medical electrical equipment - Part 2-25: Particular requirements for the basic safety and essential performance of electrocardiographs," Oct. 2011.

[3] Y.-P. Chen, D. Jeon, Y. Lee, Y. Kim, Z. Foo, I. Lee, N. B. Langhals, G. Kruger, H. Oral, O. Berenfeld, Z. Zhang, D. Blaauw, and D. Sylvester, "An injectable 64 nw ecg mixed-signal soc in 65 nm for arrhythmia monitoring," *IEEE Journal of Solid-State Circuits*, vol. 50, no. 1, pp. 375–390, 2015.

[4] B. Mishra, N. Arora, and Y. Vora, "Wearable ECG for real time complex P-QRS-T detection and classification of various arrhythmias," in *2019 11th International Conference on Communication Systems & Networks (COMSNETS)*, pp. 870–875, 2019.

[5] K.-R. Lee, J. Kim, C. Kim, D. Han, J. Lee, J. Lee, H. Jeong, and H.-J. Yoo, "A 1.02 μW/ STT-MRAM-based DNN ECG arrhythmia monitoring SoC with leakage-based delay MAC unit," *IEEE Solid-State Circuits Letters*, vol. 3, pp. 390–393, 2020.

[6] Y.-P. Hsu, Z. Liu, and M. M. Hella, "A 1.8 μW -65 dB THD ECG acquisition front-end IC using a bandpass instrumentation amplifier with Class-AB output configuration," *IEEE Transactions on Circuits and Systems II: Express Briefs*, vol. 65, no. 12, pp. 1859–1863, 2018.

[7] Y. Li, A. L. Mansano, Y. Yuan, D. Zhao, and W. A. Serdijn, "An ECG recording front-end with continuous-time level-crossing sampling," *IEEE Transactions on Biomedical Circuits and Systems*, vol. 8, pp. 626–635, Oct. 2014.

[8] S. Maji and M. J. Burke, "Establishing the input impedance requirements of ecg recording amplifiers," *IEEE Transactions on Instrumentation and Measurement*, vol. 69, no. 3, pp. 825–835, 2020.

[9] G. Lenis, N. Pilia, A. Loewe, W. H. W. Schulze, and O. Dössel, "Comparison of baseline wander removal techniques considering the preservation of ST changes in the ischemic ECG: a simulation study," *Computational and Mathematical Methods in Medicine*, vol. 2017, pp. 1–13, 03 2017.

[10] C. Böck, P. Kovács, P. Laguna, J. Meier, and M. Huemer, "Ecg beat representation and delineation by means of variable projection," *IEEE Transactions on Biomedical Engineering*, vol. 68, no. 10, pp. 2997–3008, 2021.

[11] N. Arora and B. Mishra, "Origins of ECG and evolution of automated DSP techniques: a review," *IEEE Access*, vol. 9, pp. 140853–140880, 2021.

[12] J. R. Hampton, *The ECG made easy*. Elsevier, 2013.

[13] Q. Fan, F. Sebastiano, J. H. Huijsing, and K. A. A. Makinwa, "A 1.8 μW 60 nV/$\sqrt{Hz}$ capacitively-coupled chopper instrumentation amplifier in 65 nm CMOS for wireless sensor nodes," *IEEE Journal of Solid-State Circuits*, vol. 46, no. 7, pp. 1534–1543, 2011.

[14] T. C. Carusone, D. A. Johns, and K. W. Martin, *Analog Integrated Circuit Design*, ch. 9, pp. 392–394. John Wiley and Sons, Inc., 2012.